



Cite this: *RSC Adv.*, 2017, 7, 47143

Rapid and label-free strategy for the sensitive detection of Hg^{2+} based on target-triggered exponential strand displacement amplification†

Chang Yeol Lee,^a Hyo Yong Kim,^a Jun Ki Ahn,^a Ki Soo Park ^{*b}
and Hyun Gyu Park ^{*a}

We herein describe a rapid and label-free strategy for the sensitive detection of Hg^{2+} based on target-triggered exponential strand displacement amplification (eSDA). The developed strategy utilizes specially designed DNA probes that form mismatched thymine–thymine (T–T) base pairs at their 3′-ends. In the absence of Hg^{2+} , the mismatched T–T base pairs prohibit the DNA polymerase-mediated extension and the subsequent eSDA does not occur. On the other hand, the presence of Hg^{2+} that mediates the formation of stable T– Hg^{2+} –T base pairs, enables the extension of DNA probes by DNA polymerase. As a result, a large number of duplexes are produced through the eSDA, which is simply monitored in real-time by the gradual fluorescence enhancement from SYBR green I. By employing this strategy, we detected Hg^{2+} down to 2.95 pM within 30 min, and the practical applicability of this method was successfully demonstrated by detecting Hg^{2+} in tap water.

Received 21st August 2017
Accepted 29th September 2017

DOI: 10.1039/c7ra09226a

rsc.li/rsc-advances

Introduction

As one of the most dangerous heavy metal ions, Hg^{2+} has been a serious threat to human health because it can be accumulated in human bodies and lead to damage in the brain and the nervous, kidney, and endocrine systems.^{1,2} To prevent its deleterious effects, the accurate detection of Hg^{2+} has long been required and numerous methods have been developed based on the specific interaction between Hg^{2+} and a mismatched thymine–thymine (T–T) base pair.³ The examples of this type are found in different systems which rely on electrochemistry,^{4,5} colorimetry,^{6–8} and fluorometry.^{9–19}

Notably, the fluorometric methods which operate in a reliable and simple manner, have been extensively investigated. For instance, Deng *et al.* utilized fluorescent silver nanoclusters for the detection of Hg^{2+} and Qi *et al.* developed a fluorescent method for Hg^{2+} based on the target-induced activation of deoxyribozyme activity.^{11,12} In addition, several sensing strategies were also made in combination with isothermal signal amplification methods including HCR, hyperbranched RCA, and EXPAR.^{15,16,19} Although promising, they not only exhibit the

poor sensitivity, but also require the labeling with fluorophore and quencher, preparation and functionalization of nano-materials, and long detection time, hampering their practical use (Table S1†). Therefore, it is highly necessary to develop a new detection strategy for Hg^{2+} that overcomes the drawbacks of the previous systems including high-cost, poor sensitivity, and complicated and long procedures.

Towards this goal, we herein developed a rapid and label-free strategy for the sensitive detection of Hg^{2+} based on target-triggered exponential strand displacement amplification (eSDA), an isothermal nucleic acid amplification method that rapidly produces a large number of duplexes through the cooperative actions of DNA polymerase and nicking endonuclease.^{20–22} In principle, DNA probes that form the mismatched T–T base pairs at their 3′-ends, are stabilized by the presence of Hg^{2+} through the formation of stable T– Hg^{2+} –T base pairs, which enables the extension of DNA probes by DNA polymerase. As a result, eSDA is initiated to produce a large number of duplex products, which is simply monitored in real-time by the gradual fluorescence enhancement from a double-stranded (ds) DNA specific fluorescent dye, SYBR green I. Based on this novel strategy, Hg^{2+} was rapidly analyzed with the high sensitivity and selectivity and its practical applicability was demonstrated by accurately detecting Hg^{2+} present in tap water.

Experimental

Materials

All DNA strands used in the study were synthesized by Genotech Co. (Daejeon, South Korea) and purified by desalting, except for

^aDepartment of Chemical and Biomolecular Engineering (BK 21+ Program), KAIST, Daehak-ro 291, Yuseong-gu, Daejeon 305-338, Republic of Korea. E-mail: hgpark@kaist.ac.kr; Fax: +82-42-350-3910; Tel: +82-42-350-3932

^bDepartment of Biological Engineering, College of Engineering, Konkuk University, Seoul 05029, Republic of Korea. E-mail: kskonkuk@gmail.com; Fax: +82-2-450-3742; Tel: +82-2-450-3742

† Electronic supplementary information (ESI) available. See DOI: 10.1039/c7ra09226a

TP (purified by PAGE). The sequences of all DNAs are listed in Table S2.† Klenow fragment (3' → 5' exo-) (KF) and Nt.AlwI were purchased from New England Biolabs Inc. (Beverly, MA, USA). The metal salts and SYBR green I were purchased from Sigma-Aldrich (St. Louis, MO, USA). All other chemicals were of analytical grade and used without further purification. Ultra-pure DNase/RNase-free distilled water (DW) purchased from Bioneer® (Daejeon, Korea) was used in all the experiments.

Hg²⁺ detection procedure

28.5 μL of DW, 2 μL of TP (2.5 μM), 2 μL of FP-T12 (2.5 μM), 2 μL of RP (2.5 μM), 4 μL of dNTP (2.5 mM), 2.5 μL of SYBR green I (20×), 1 μL of KF (5 U μL⁻¹), 1 μL of Nt.AlwI (10 U μL⁻¹), 2 μL of Hg(NO₃)₂ at varying concentrations and 5 μL of NEBuffer 4 (20 mM Tris-acetate, 50 mM potassium acetate, 10 mM magnesium acetate, 1 mM DTT, pH 7.9 at 1× concentration) were mixed to prepare the reaction solutions of 50 μL and their fluorescence was measured in real-time at every 30 s at 42.5 °C during eSDA on C1000™ thermal cycler (Bio-Rad, CA, USA).²³

Detection of Hg²⁺ in tap water (4%)

The tap water was first confirmed to be free of Hg²⁺ with the standard method, inductively coupled plasma-mass spectrometry (ICP-MS) (Fig. S1†). Then, Hg²⁺ at varying concentrations was spiked into the tap water, which was subsequently analyzed using the same procedure to detect Hg²⁺ as described above.

Results and discussion

The basic principle of the new strategy to detect Hg²⁺ is illustrated in Fig. 1, which relies on target-triggered eSDA. The developed strategy utilizes the specially designed DNA probes composed of template, forward primer and reverse primer. Forward primer (FP) and template (TP) are designed to form the mismatched T-T base pairs at their 3'-ends. In addition, FP and reverse primer (RP) bear the sequence that contains a single-stranded (ss) recognition site for nicking endonuclease (Nt.AlwI) at their 5'-ends. In the absence of Hg²⁺, FP, TP, and RP coexist separately due to the mismatched T-T base pairs and the subsequent eSDA does not take place. On the contrary, the presence of Hg²⁺ enables FP and TP to hybridize at their 3'-ends through the formation of stable T-Hg²⁺-T base pairs, which promotes the extension from their 3'-ends by DNA polymerase (Klenow fragment (KF)) so that the double-stranded (ds) recognition site for nicking endonuclease is formed (Fig. S2†).^{16,24} Thus, the nicking endonuclease cleaves FP at the fourth base downstream from the recognition site and generates a new initiation site for the next round of extension, from which ss extension products (TP1) are displaced by DNA polymerase. This cycle termed SDA I consisting of cleavage, extension, and displacement continuously produces a lot of ssDNAs (TP1). Importantly, Hg²⁺ is released in the extension accompanying the displacement during SDA I and recycled to promote another cycle of SDA I.^{19,25} In addition, TP1 generated in SDA I, contains the sequence complementary to the 3'-end of RP and thus forms the hybridization complex with RP, which is extended by DNA polymerase from its 3'-ends to generate the ds

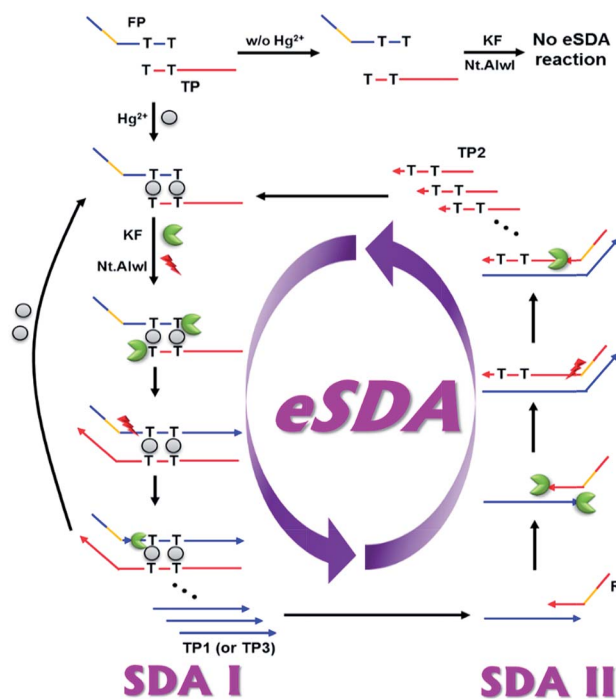


Fig. 1 Schematic illustration of the Hg²⁺ detection method based on target-triggered eSDA. TP and TP1 are only involved in the first cycle of SDA I and SDA II, respectively. The orange color in FP and RP indicates the single-stranded recognition sequence for nicking endonuclease (Nt.AlwI) and the arrow shows the 3'-end of all DNA probes.

recognition site for nicking endonuclease. In the same manner to SDA I, a large number of ss extension products (TP2) containing T bases are produced through SDA II, which induces the formation of the hybridization complex between TP2 and FP and promotes SDA I to produce TP3 continuously. It is fed back to SDA II through which a large number of TP2s are generated again. Likewise, SDA I and II are cooperatively repeated to promote the exponential amplification (eSDA) generating a large number of duplex products, which is simply monitored in real-time by the gradual fluorescence enhancement from SYBR green I.

Considering that the number of mismatched T-T base pairs, reaction temperature, and concentration of primers would have significant effects on the detection of Hg²⁺, these factors were first optimized by examining the time-dependent fluorescence enhancement from SYBR green I. The results of experiments in which the number of mismatched T-T base pairs, reaction temperature, and concentration of primers were varied, showed that 12 of mismatched T-T base pairs, 42.5 °C of reaction temperature, and 100 nM of primers were ideal to achieve the best detection performance. Thus, these optimal conditions were used for further experiments (Fig. 2). It should be noted that the nonspecific background signal was inevitably produced in the absence of Hg²⁺, which might be due to the *ab initio* DNA synthesis, the template DNA-independent polymerization of free nucleotides by DNA polymerase.^{26,27}

Under the optimal conditions, we measured the time-dependent fluorescence enhancement from SYBR green I at varying concentrations of Hg²⁺ (Fig. 3(a)). For the accurate



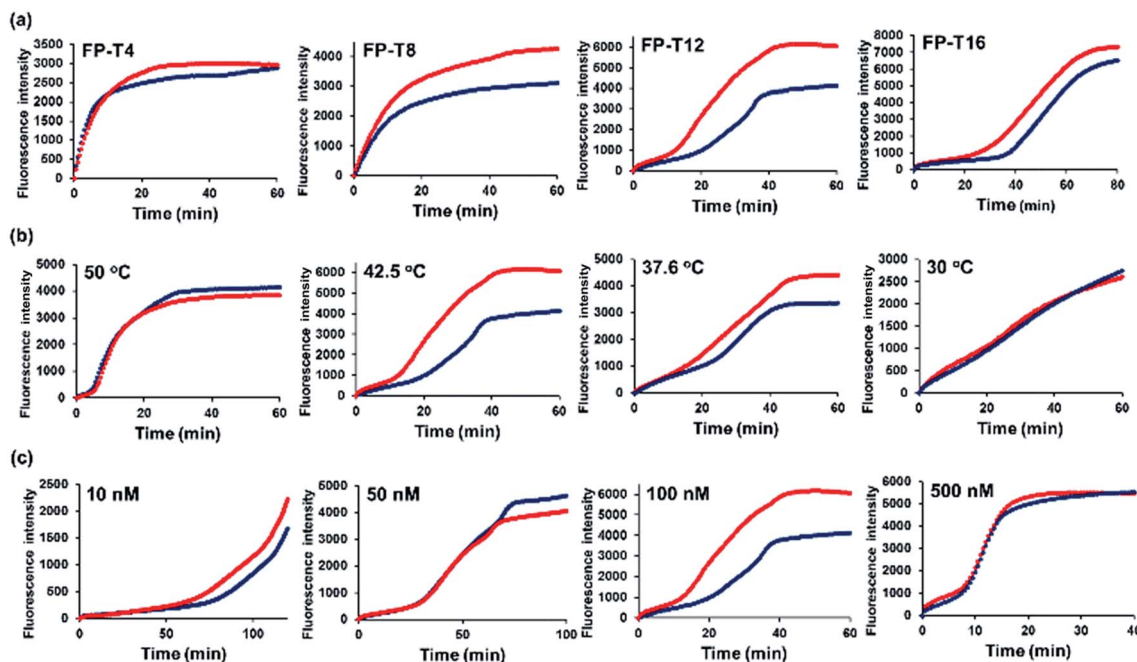


Fig. 2 Optimization of the reaction conditions for the Hg^{2+} detection method. Fluorescence intensities from SYBR green I are plotted as a function of time during target-triggered eSDA in the absence (blue) and presence (red) of Hg^{2+} (10 nM). The corresponding reaction conditions are indicated at the left upper corner of each graph. (a) Optimization of the number of mismatched T–T base pairs (Table S2†). The reaction temperature is 42.5 °C and the concentration of primers is 100 nM. (b) Optimization of the reaction temperature. The number of mismatched T–T base pairs is 12 and the concentration of primers is 100 nM. (c) Optimization of the concentration of primers. The number of mismatched T–T base pairs is 12 and the reaction temperature is 42.5 °C.

quantification of Hg^{2+} , threshold time (T_t), the time to reach the threshold fluorescence intensity, was defined. The results in Fig. 3(a) showed that T_t decreased with increasing concentrations of Hg^{2+} , and the entire assay was completed less than 30 min. In addition, the plot of T_t vs. logarithm of Hg^{2+} concentration showed that an excellent linear relationship ($T_t = -3.7044 \times \log_{10}(C_{\text{Hg}^{2+}}/\text{pM}) + 31.631$, $R^2 = 0.9911$) existed in the range of 10 pM to 10 nM and the limit of detection (LOD) was calculated to be 2.95 pM based on $3 \sigma/S$, where σ is the standard deviation (SD) of blank and S is the slope of the linear relationship (Fig. 3(b)).^{28,29} This LOD value is lower than those from the previous reports to detect Hg^{2+} (Table S1†).^{11–16,18} The relative standard deviations (RSDs) were also calculated at varying

concentrations of Hg^{2+} . The results in Table S3† showed that they were less than 10%, proving the good reproducibility of this method.³⁰ These results indicate that target-triggered eSDA with the efficient amplification ability could be exploited to sensitively and reliably analyze Hg^{2+} .

To evaluate the specificity of the present strategy towards Hg^{2+} , the abilities of other metal ions (Ca^{2+} , Fe^{3+} , Co^{2+} , Ni^{2+} , Cu^{2+} , Zn^{2+} , Ag^+ , Cd^{2+} , and Pb^{2+}) to induce the decrease of T_t , were examined and compared with that from Hg^{2+} . As shown in Fig. 4, the significant decrease of T_t was observed in the presence of Hg^{2+} while the effects of other metal ions on T_t were negligible even though they were applied at a hundred times higher concentration than that of Hg^{2+} . These results clearly demonstrate that this

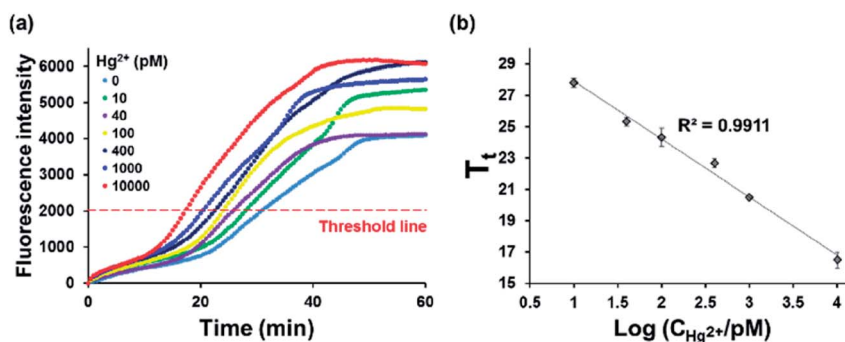


Fig. 3 Sensitivity of the Hg^{2+} detection method. (a) Fluorescence intensities from SYBR green I are plotted as a function of time during target-triggered eSDA in the presence of varying concentrations of Hg^{2+} . The threshold fluorescence intensity was set for 2000. (b) Linear relationship between T_t and logarithm of Hg^{2+} concentration (10 pM to 10 nM).



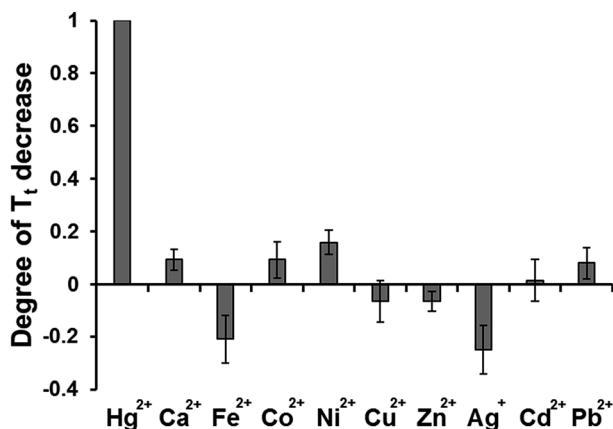


Fig. 4 Specificity of the Hg^{2+} detection method. Degrees of T_t decrease in the presence of Hg^{2+} (10 nM) and different metal ions (1 μM). Degree of T_t decrease is defined as $(T_{t,\text{blank}} - T_{t,\text{M}})/(T_{t,\text{blank}} - T_{t,\text{Hg}^{2+}})$, where $T_{t,\text{blank}}$, $T_{t,\text{M}}$, and $T_{t,\text{Hg}^{2+}}$ are the threshold times in the presence of blank, metal ions, and Hg^{2+} , respectively.

Table 1 Determination of Hg^{2+} in the tap water^a

Added Hg^{2+} (nM)	Measured Hg^{2+b} (nM)	Recovery ^c (%)
0	Not detected	—
0.5	0.45	89.3
5	5.21	104.1

^a The concentrations of Hg^{2+} were determined based on the standard curve established by the detection of Hg^{2+} in the buffer solution (Fig. 3(b)). Based on this calibration curve, T_t values from unknown samples were used to determine the concentration of Hg^{2+} in the tap water. ^b Mean of three measurements. ^c Measured value/added value $\times 100$.

system is highly selective to Hg^{2+} , indicating that target-triggered eSDA is exclusively initiated by the formation of specific and stable T- Hg^{2+} -T base pairs.

Finally, the practical applicability of the proposed method was verified by determining Hg^{2+} spiked in tap water. The results in Fig. S3(a)† confirmed that T_t value obtained from the tap water was the same with that from the buffer solution, indicating that the developed system is insensitive to interfering substances present in the tap water. Therefore, the concentrations of Hg^{2+} were determined based on the standard curve established by the detection of Hg^{2+} in the buffer solution (Fig. 3(b)). As presented in Table 1 and Fig. S3(b),† Hg^{2+} concentrations were successfully determined with the excellent precision, as evidenced by the recovery rates (89.3% and 104.1%). These results clearly confirm that the developed strategy can be used to determine Hg^{2+} in real samples.

Conclusions

In summary, we developed a rapid and label-free method for the sensitive detection of Hg^{2+} based on target-triggered eSDA. By taking advantage of the efficient amplification ability of eSDA and real-time signal acquisition, the present strategy could

detect sHg^{2+} down to 2.95 pM within 30 min, which outperforms the previous fluorometric methods. In addition, its practical applicability was successfully demonstrated by its use to determine Hg^{2+} in the tap water. Importantly, this strategy does not require the labeling with fluorophore and quencher and preparation and functionalization of nanomaterials, eliminating the drawbacks of previous fluorometric systems including complexity and high-cost. To the best of our knowledge, this is the first report to exploit the eSDA for the sensitive determination of metal ions, which would broaden the application scope of eSDA as a novel analytical tool.

Conflicts of interest

There are no conflicts to declare.

Acknowledgements

This work was supported by the Mid-career Researcher Support Program through the National Research Foundation (NRF) funded by the Ministry of Science, ICT & Future planning (MSIP) of Korea (No. 2015R1A2A1A01005393) and by the Center for BioNano Health-Guard funded by the MSIP of Korea as Global Frontier Project (Grant H-GUARD_2013M3A6B2078964). Financial support was also provided by the NRF grant funded by the MSIP of Korea (No. 2017R1C1B5017724).

Notes and references

- 1 P. B. Tchounwou, W. K. Ayensu, N. Ninashvili and D. Sutton, *Environ. Toxicol.*, 2003, **18**, 149–175.
- 2 F. Zahir, S. J. Rizwi, S. K. Haq and R. H. Khan, *Environ. Toxicol. Pharmacol.*, 2005, **20**, 351–360.
- 3 Y. Miyake, H. Togashi, M. Tashiro, H. Yamaguchi, S. Oda, M. Kudo, Y. Tanaka, Y. Kondo, R. Sawa and T. Fujimoto, *J. Am. Chem. Soc.*, 2006, **128**, 2172–2173.
- 4 C. Tortolini, P. Bollella, M. L. Antonelli, R. Antiochia, F. Mazzei and G. Favero, *Biosens. Bioelectron.*, 2015, **67**, 524–531.
- 5 G. Wang, H. Huang, X. Zhang and L. Wang, *Biosens. Bioelectron.*, 2012, **35**, 108–114.
- 6 Q. Zhang, Y. Cai, H. Li, D.-M. Kong and H.-X. Shen, *Biosens. Bioelectron.*, 2012, **38**, 331–336.
- 7 W. Ren, Y. Zhang, W. T. Huang, N. B. Li and H. Q. Luo, *Biosens. Bioelectron.*, 2015, **68**, 266–271.
- 8 S. Liu, X. Leng, X. Wang, Q. Pei, X. Cui, Y. Wang and J. Huang, *Microchim. Acta*, 2017, **184**, 1969–1976.
- 9 J. Ge, Y.-H. Du, J.-J. Chen, L. Zhang, D.-M. Bai, D.-Y. Ji, Y.-L. Hu and Z.-H. Li, *Sens. Actuators, B*, 2017, **249**, 189–194.
- 10 J. Ge, X.-P. Li, J.-H. Jiang and R.-Q. Yu, *Talanta*, 2014, **122**, 85–90.
- 11 L. Deng, Z. Zhou, J. Li, T. Li and S. Dong, *Chem. Commun.*, 2011, **47**, 11065–11067.
- 12 L. Qi, Y. Zhao, H. Yuan, K. Bai, Y. Zhao, F. Chen, Y. Dong and Y. Wu, *Analyst*, 2012, **137**, 2799–2805.
- 13 D. Huang, C. Niu, X. Wang, X. Lv and G. Zeng, *Anal. Chem.*, 2013, **85**, 1164–1170.



- 14 G. Wang, G. Xu, Y. Zhu and X. Zhang, *Chem. Commun.*, 2014, **50**, 747–750.
- 15 J. Huang, X. Gao, J. Jia, J.-K. Kim and Z. Li, *Anal. Chem.*, 2014, **86**, 3209–3215.
- 16 H. Jia, Z. Wang, C. Wang, L. Chang and Z. Li, *RSC Adv.*, 2014, **4**, 9439–9444.
- 17 G. Zhu, Y. Li and C.-y. Zhang, *Chem. Commun.*, 2014, **50**, 572–574.
- 18 X. Zhu, X. Zhou and D. Xing, *Biosens. Bioelectron.*, 2011, **26**, 2666–2669.
- 19 J. Chen, P. Tong, Y. Lin, W. Lu, Y. He, M. Lu, L. Zhang and G. Chen, *Analyst*, 2015, **140**, 907–911.
- 20 G. T. Walker, M. S. Fraiser, J. L. Schram, M. C. Little, J. G. Nadeau and D. P. Malinowski, *Nucleic Acids Res.*, 1992, **20**, 1691–1696.
- 21 C. Shi, Q. Liu, M. Zhou, H. Zhao, T. Yang and C. Ma, *Sens. Actuators, B*, 2016, **222**, 221–225.
- 22 C. Shi, Q. Liu, C. Ma and W. Zhong, *Anal. Chem.*, 2013, **86**, 336–339.
- 23 K. S. Park, C. Y. Lee and H. G. Park, *Chem. Commun.*, 2015, **51**, 9942–9945.
- 24 K. S. Park, C. Jung and H. G. Park, *Angew. Chem., Int. Ed.*, 2010, **49**, 9757–9760.
- 25 X. Zhou, Q. Su and D. Xing, *Anal. Chim. Acta*, 2012, **713**, 45–49.
- 26 N. V. Zyrina, V. N. Antipova and L. A. Zheleznya, *FEMS Microbiol. Lett.*, 2014, **351**, 1–6.
- 27 E. Tan, B. Erwin, S. Dames, T. Ferguson, M. Buechel, B. Irvine, K. Voelkerding and A. Niemz, *Biochemistry*, 2008, **47**, 9987–9999.
- 28 Y. L. Huang, Z. F. Gao, H. Q. Luo and N. B. Li, *Sens. Actuators, B*, 2017, **238**, 1017–1023.
- 29 K. Wang, J. Liao, X. Yang, M. Zhao, M. Chen, W. Yao, W. Tan and X. Lan, *Biosens. Bioelectron.*, 2015, **63**, 172–177.
- 30 M. Mei, X. Huang, K. Liao and D. Yuan, *Anal. Chim. Acta*, 2015, **860**, 29–36.

